Artificial spectral filtering in dissipative soliton fiber lasers with invisible bandpass filters*

Kong Ling-Jie(孔令杰), Xiao Xiao-Sheng(肖晓晟), and Yang Chang-Xi(杨昌喜)†

State Key Laboratory of Precision Measurement Technology and Instruments, Department of Precision Instruments, Tsinghua University, Beijing 100084, *China*

(Received 19 December 2011; revised manuscript received 14 May 2012)

We numerically study the artificial spectral-filtering effect in dissipative soliton fiber lasers without intracavity spectral filter. It is found that in the dissipative soliton lasers with real saturable absorbers (SAs), the dynamic spectral filtering of the real SAs serves as an artificial spectral filter and contributes to the pulse shaping. While in the dissipative soliton lasers with artificial SAs, such as nonlinear polarization rotation, the spectral filtering introduced by the intracavity polarization-dependent components acts as an artificial spectral filter and shapes the pulses to get mode-locking. The investigation of the artificial spectral-filtering effect reveals the operating mechanisms of the dissipative soliton fiber lasers without visible bandpass filter.

Keywords: fiber laser, mode locking

PACS: 42.55.Wd, 42.60.Fc **DOI:** 10.1088/1674-1056/21/9/094210

1. Introduction

Ultrafast fiber lasers have advantages over the solid-state lasers in compactness, robustness, and low cost. So far, many techniques have been proposed to improve the performance of mode-locked fiber lasers,[1] such as soliton fiber lasers, stretched-pulse fiber lasers, and self-similar fiber lasers. The nonlinear phase shifts are managed in various ways to achieve a high pulse energy. Recently, the novel dissipative soliton fiber lasers, also named as the all-normal-dispersion (ANDi) fiber lasers, have been proposed,[2,3] which are promising to provide performances comparable to those of the solid-state femtosecond lasers. Different from the previous lasers, they rely on the dissipative processes to compensate the nonlinear phase and avoid the wave breaking.[4] So far, sub-100 fs pulses at watt-level powers from single mode fibers have been reported in ANDi fiber lasers.[5]

Theoretical studies have pointed out that the spectral filtering plays a critical role in achieving high energy pulses in the dissipative soliton fiber lasers.[4,6] The spectral filter converts the frequency chirp to the self-amplitude modulation (SAM). It is found that the output spectral shape evolves gradually with the decreasing spectral-filter bandwidth (BW) from the parabolic-top spectrum to the fringed and broadened spectrum. This indicates that the spectral filters affect the operating mechanisms of the dissipative soliton fiber lasers.[7] Generally, most intracavity components, such as the wavelength division multiplexer and the fiber coupler, have such broad BWs that they can be regarded to be wavelength-independent for the mode-locking pulses. So for the stable mode-locking, the bandpass filters are usually required to provide enough SAM.

However, several ANDi fiber lasers without intentional filter have been reported. With real saturable absorbers (SAs), such as semiconductor saturable absorber (SESAM),[8] carbon nanotube (CNT),[9] and grapheme,[10] ANDi fiber lasers without intracavity filter have been demonstrated. Our group and Zhao *et al.* also have reported ANDi lasers mode-locked by aritificial SA–nonlinear polarization rotation (NPR),[11−13] where no real bandpass filters were inserted in the cavity. To improve the performance of such dissipative soliton fiber lasers without visible filter, the underlying mechanisms of mode-locking should be understood. However, to the best of our knowledge, no theoretical explanation has been proposed.

*Project supported by the National Natural Science Foundation of China (Grant No. 61077032).

†Corresponding author. E-mail: cxyang@tsinghua.edu.cn

© 2012 Chinese Physical Society and IOP Publishing Ltd

In this paper, we numerically study the mode-locking in the dissipative soliton fiber lasers without visible bandpass filter. An artificial spectral-filtering effect is found in lasers with real and artificial SAs. Different from the lasers with the conventional filters, the dynamic spectral filtering is found in the lasers with real SAs (such as SESAM, CNT, and graphene) and without visible filter. Meanwhile, in the NPR-based dissipative soliton lasers without visible filter, it is found that an artificial spectral filtering will be introduced by the polarization-dependent components.

2. Simulation model and results

2.1. Dissipative soliton fiber lasers with real SAs and without visible spectral filter

Without the conventional spectral filters, the steady passive mode-lockings have been achieved in the dispersion-compensation-free lasers with SESAM,[8] CNT,[9] and graphene[10] as the SAs. The SESAM usually has a reflection BW as wide as 100 nm. The operating BW of the CNT determined by the tube diameter distribution is also quite broad compared to the BW of the output pulse. And the absorption of graphene is wavelength-independent due to the linear dispersion relation. So the filtering effect introduced by those SAs can be neglected in the reports.[8−10]

In the following, numerical simulations based on the scalar model of the fiber lasers are carried out. And the SA is found to show a dynamic spectral-filtering effect.

The simulated laser consists of a segment of single mode fiber (SMF1), a Yb-doped fiber, and another single mode fiber (SMF2) in order, which is similar to that in Ref. [7]. The pulse propagation in these fiber sections is modeled by

$$\frac{\partial A}{\partial z} = gA - \mathrm{i}\frac{\beta_2}{2}\frac{\partial^2 A}{\partial \tau^2} + \frac{\beta_3}{6}\frac{\partial^3 A}{\partial \tau^3} + \mathrm{i}\gamma|A|^2 A, \quad (1)$$

where A is the electrical field envelope, z is the propagating coordinate, τ is the local time, β_2 is the group velocity dispersion, β_3 is the third-order dispersion, and γ is the nonlinear coefficient. The gain coefficient is defined as

$$g = \frac{g_0}{1 + \int_{-T_\mathrm{R}/2}^{T_\mathrm{R}/2} |A|^2 \mathrm{d}t / E_\mathrm{sat}}, \quad (2)$$

where g_0 is the small-signal gain, E_sat is the saturation energy, and T_R is the cavity round-trip time. Different from the gain-guided soliton fiber laser, in which the Er-doped fiber has a narrow gain bandwidth, the gain dispersion of the Yb-doped fiber can be neglected due to its broad fluorescent bandwidth. Here the −3 dB bandwidth of the lorentzian-shaped gain profile is 40 nm. The fiber sections are followed by an ideal SA with monotonically increasing transmission

$$T = 1 - \frac{l_0}{1 + P(\tau)/P_\mathrm{sat}}, \quad (3)$$

where $l_0 = 0.7$ is the unsaturated loss, $P(\tau)$ is the instantaneous pulse power, and P_sat is the saturation power. Before the pulses are injected into SMF1 to make a ring cavity, they go through an optical coupler (OC), and 70% of the pulse energy is dumped.

Parameters in the simulations are: 200 cm SMF1, $\beta_2 = 23$ fs^2/mm, $\beta_3 = 25.4$ fs^3/mm, $\gamma = 0.0044$ W^{-1}·m^{-1}; 50 cm Yb-doped fiber, $\beta_2 = 23.7$ fs^2/mm, $\beta_3 = 25.4$ fs^3/mm, $\gamma = 0.0048$ W^{-1}·m^{-1}, $g_0 = 3.45$ corresponding to 30 dB of small-signal gain, $E_\mathrm{sat} = 720$ pJ; 100 cm SMF2, $\beta_2 = 23$ fs^2/mm, $\beta_3 = 25.4$ fs^3/mm, $\gamma = 0.0044$ W^{-1}·m^{-1}. The simulation of Eq. (1) is carried out with the slip-step Fourier method.

The steady mode locking is achieved with the given parameters, and the output is shown in Fig. 1 with the red solid line. The output pulse energy is 1.27 nJ, the central wavelength is 1031 nm, and the −3 dB spectral bandwidth is 8.70 nm. The temporal full width at half maximum (FWHM) of the output pulse is 9.0 ps, indicating that the output pulses are highly chirped. To study the function of the SA, we also show the temporal and the spectral shapes of the pulse before the SA in Fig. 1. It can be seen that the transmissions in temporal and spectral domains are both nonuniform (more information will be shown later in Fig. 4). Furthermore, as shown with the simulated polarization gate frequency resolved optical gating (PG-FROG) in Fig. 2, the pulse gets shorter and the spectral bandwidth gets narrower after the SA, i.e., the FWHM decreases from 10.1 ps to 9.0 ps, and the −3 dB bandwidth decreases from 9.22 nm to 8.70 nm.

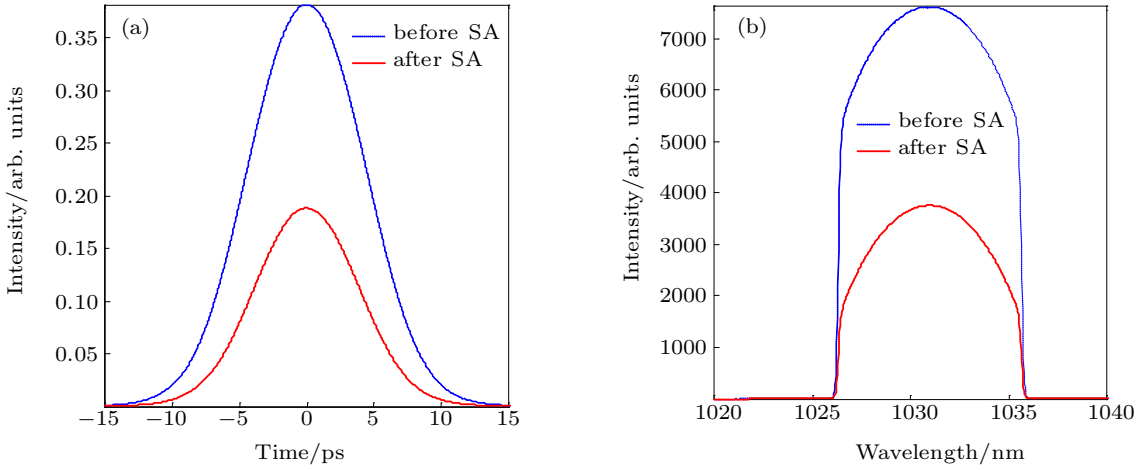


Fig. 1. (colour online) (a) Pulses and (b) the corresponding spectra before and after the SA.

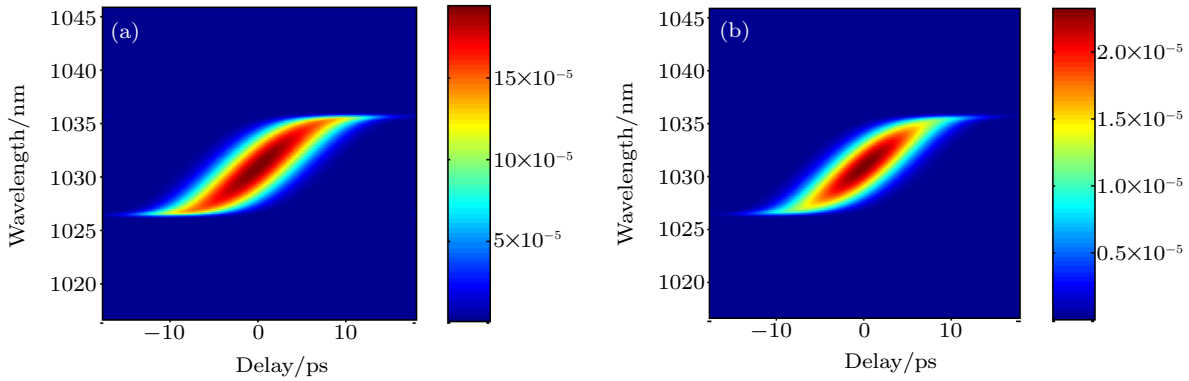


Fig. 2. (colour online) The simulated PG-FROG traces of the pulse (a) before and (b) after the SA in steady mode locking.

The intracavity dynamics of the pulse temporal FWHM and the spectral bandwidth are shown in Fig. 3. Apparently, for the highly chirped pulses, the SA here introduces an effective spectral filtering for pulse shaping and steady mode locking.[14] This is in contrast to that in Ref. [10], where the bandpass filtering is suspected to resulting from the birefringence in the long cavity laser.

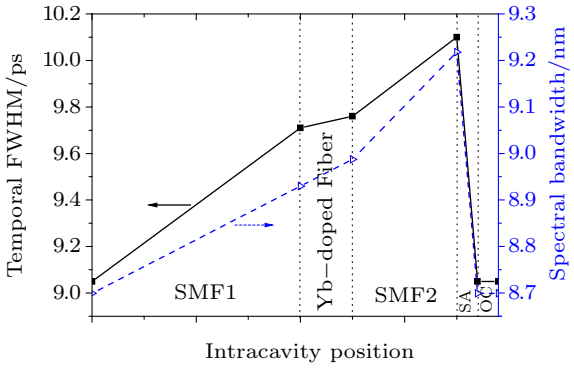


Fig. 3. (colour online) The intracavity dynamics of the pulse temporal FWHM and the spectral bandwidth.

It should be noted that different from the dissipative soliton lasers with the convential spectral filters, the spectral-filtering effect introduced by the SA is dynamic.[9] From Eq. (3), it can be seen that the transmission of the SA depends on the pulse shape, i.e., the power distribution. So in the self-starting process, the pulse shaping at the SA obtains feedback from the pulse shape. And the SA adjusts its transmission curve untill the steady mode locking is achieved. This is also confirmed in the simulation, and the results are shown in Fig. 4. The blue dash line shows one of the dynamic transmission curves of the SA in the self-starting process, and the red solid line shows the stabilized transmission curve of the SA. It can be seen that these two transmission curves are quite different. In this sense, the dynamic spectral-filtering effect makes the mode-locking complicated, which may restrict the parameter regions of steady mode-locking.

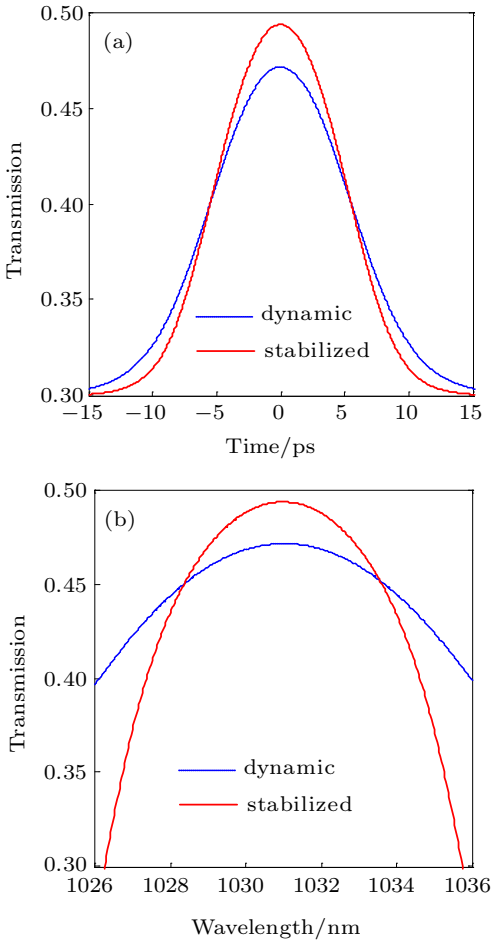


Fig. 4. (colour online) The effective filtering of the SA in (a) temporal and (b) spectral domains.

2.2. Dissipative soliton fiber lasers with artificial SAs and without visible spectral filter

The steady mode lockings have also been reported in the dissipative soliton fiber lasers with artificial SAs and with the convential spectral filter. With the ANDi fiber lasers mode-locked by NPR, our group[11,12] and Zhao *et al.*[13] have demonstrated experimentally that the dissipative soliton lasers can work with invisible intracavity bandpass filters.

The following simulation is based on the experimental setup similar to that in Ref. [15], except that no intracavity Gaussian filter is included here. The ring cavity consists of SMF1, Yb-doped fiber, SMF2, quarter waveplate (QWP1), half waveplate (HWP), polarization beam splitter (PBS), and QWP2 in order. As the laser is mode-locked by NPR, the vector model should be taken to simulate the intracavity dynamics. The pulse propagation in the fiber section is modeled with coupled Ginzburg–Landau equations, and the functions of waveplates are described with the Jones matrices. The PBS is oriented to make the x components of the injecting pulses be ejected. Details and parameters should be referred to Ref. [15].

The dissipative soliton fiber laser gets mode-locking with orientations of waveplates at $\theta_{\mathrm{QWP1}} = 0.854$, $\theta_{\mathrm{HWP}} = 2.620$, and $\theta_{\mathrm{QWP2}} = 2.458$. The steady state at the PBS is shown in Fig. 5, in which the x component is ejected by the PBS as the output. The output pulse energy is 4.18 nJ, which is ∼66.9% of the total energy at the PBS. Its central wavelength is 1031.0 nm, the −3 dB spectral bandwidth is 7.8 nm., and the temporal FWHM is 14.7 ps. Compared with the case including intracavity the 12 nm BW filters in Ref. [15], the spectrum becomes narrower, and the temporal duration becomes broader, but the time–bandwidth product becomes larger.

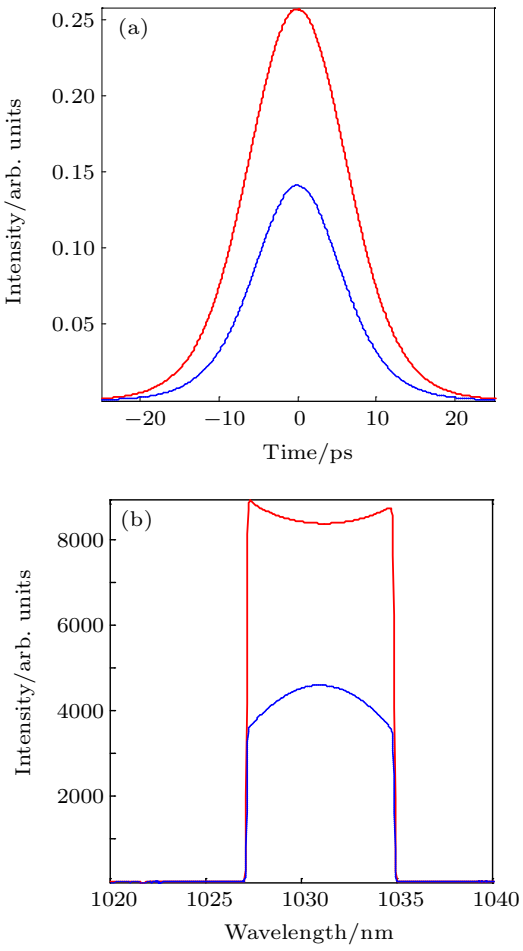


Fig. 5. (colour online) (a) Pulses and (b) the corresponding spectra at the PBS. Red solid and blue dash solid lines show the x and the y polarization components, respectively.

Different from that in the soliton fiber lasers,[16] the frequency chirp causes the polarization nonuniformity across the pulse envelope in the dissipative soliton lasers mode-locked by NPR.[15] To study the nonlinear polarization dynamics, we represent the polarization states at every time slice with points on the surface of the Poincare sphere. In Fig. 6, the polarization state traces are shown at different intracavity locations. The red open triangle represents the time slice at the peak of the pulse transmitted by the PBS, and the blue solid circle represents the time slice at 1/10 intensity of the peak of the pulse. It can be seen that the NPR happens in the fiber section, and different parts of the pulse get different polarization rotations due to their various intensities. The following QWP1 and HWP further adjust the polarization states for the pulse shaping at the PBS and getting steady mode locking. As the pulses are highly chirped, different wavelength components are of different polarization states. When the pulses go through the PBS, the transmission will vary for different wavelengths.[17] The artificial SA effect is shown in Fig. 7(a), and the spectral filtering is shown in Fig. 7(b).

Thus, the mode locking of such dissipative soliton fiber lasers can be attributed to the NPR effect, where the polarization dependent component acts as the spectral filter. Besides, from the simulations, we find that in such lasers, it is hard to work at low coupling ratios, in which the broader spectrum can be expected.[15]

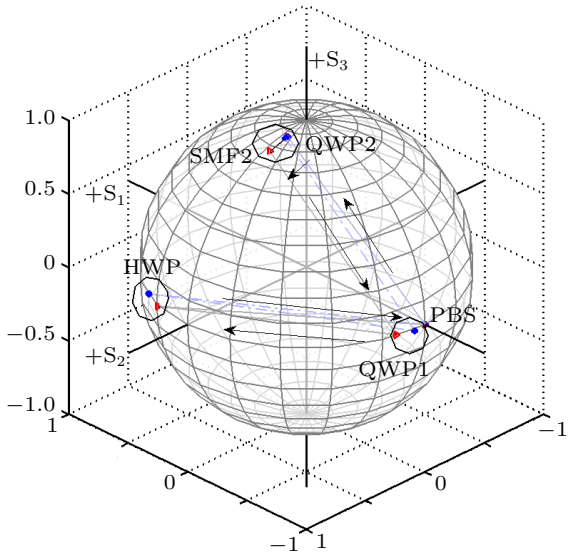


Fig. 6. (colour online) Polarization state traces at different intracavity locations (within black circle) .

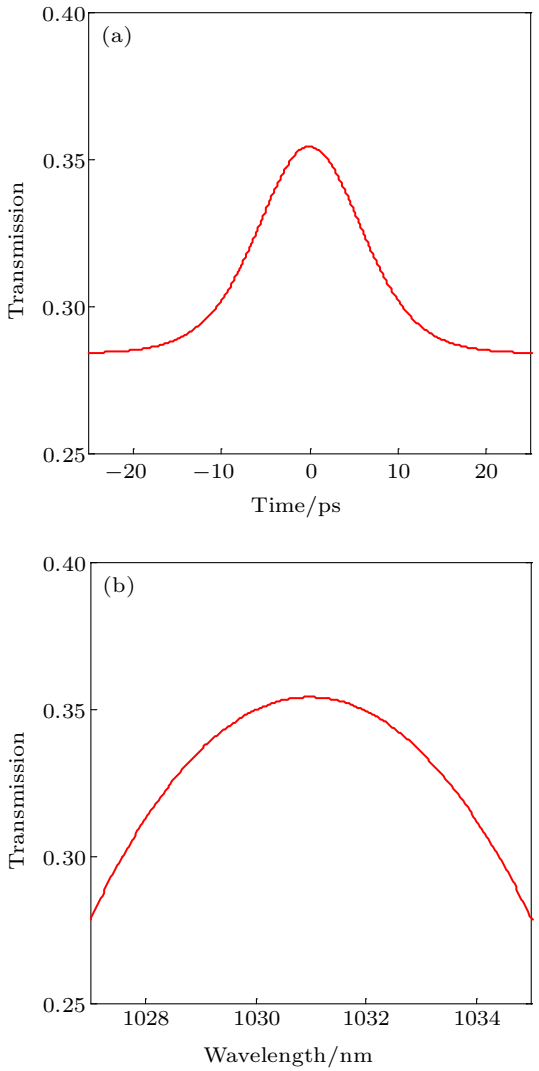


Fig. 7. Transmission curves of the PBS in (a) temporal and (b) spectral domains.

3. Conclusion

In conclusion, the artificial spectral filtering is numerically studied in the dissipative soliton fiber lasers without visible bandpass filter. It is found that in the dissipative soliton lasers with real SAs (such as SESAM, CNT, and grapheme), the dynamic spectral filtering of the real SAs plays the key role of pulse shaping. And in the dissipative soliton lasers with artificial SAs, such as NPR, the spectral filtering introduced by the intracavity polarization-dependent components shapes the pulses. These artificial spectral-filtering effects reveal the operating mechanisms of the dissipative soliton fiber lasers, which are demonstrated experimentally with invisible filters.

Acknowledgement

Kong Ling-Jie thanks W. H. Renninger and L. M. Zhao for helpful discussion.

References

[1] Wise F, Chong A and Renninger W 2008 *Laser & Photonics Rev.* **2** 58
[2] Zhao L, Tang D and Wu J 2006 *Opt. Lett.* **31** 1788
[3] Chong A, Buckley J, Renninger W and Wise F 2006 *Opt. Express* **14** 10095
[4] Renninger W, Chong A and Wise F 2008 *Phys. Rev.* A **77** 023814
[5] Kieu K, Renninger W, Chong A and Wise F 2009 *Opt. Lett.* **34** 593
[6] Bale B, Kutz J, Chong A, Renninger W and Wise F 2008 *J. Opt. Soc. Am.* B **25** 1763
[7] Chong A, Renninger W and Wise F 2008 *J. Opt. Soc. Am.* B **25** 140
[8] Tian X, Tang M, Shum P, Gong Y, Lin C, Fu S and Zhang T 2009 *Opt. Lett.* **34** 1432
[9] Kelleher E, Travers J, Sun Z, Rozhin A, Ferrari A, Popov S and Taylor J 2009 *Appl. Phys. Lett.* **95** 111108
[10] Zhao L, Tang D, Zhang H, Wu X, Bao Q and Loh K 2010 *Opt. Lett.* **35** 3622
[11] Kong L, Xiao X and Yang C 2010 *Chin. Phys.* B **19** 074212
[12] Kong L, Xiao X and Yang C 2010 *Laser Phys. Lett.* **7** 359
[13] Zhao L, Tang D, Wu X and Zhang H 2010 *Opt. Lett.* **35** 2756
[14] Renninger W, Chong A and Wise F 2011 *IEEE J. Sel. Top. Quantum Electron* 18 389
[15] Kong L, Xiao X and Yang C 2011 *Opt. Express* **19** 18339
[16] Wu J, Tang D, Zhao L and Chan C 2006 *Phys. Rev.* E **74** 046605
[17] Zhang P, Fan W, Wang X and Lin Z 2011 *Acta Phys. Sin.* **60** 024206 (in Chinese)